Photoemission Study of the Morphology and Barrier Heights at the Interface between Benz[a]anthracene and Noble Metal (111) Surfaces

ARTICLE *in* THE JOURNAL OF PHYSICAL CHEMISTRY C · AUGUST 2012

Impact Factor: 4.77 · DOI: 10.1021/jp305998b

2 AUTHORS:

Kedar Manandhar
University of Illinois at Chicago
20 PUBLICATIONS **90** CITATIONS
SEE PROFILE

Bruce A Parkinson
University of Wyoming
251 PUBLICATIONS **7,087** CITATIONS
SEE PROFILE

THE JOURNAL OF PHYSICAL CHEMISTRY C

Article

pubs.acs.org/JPCC

Photoemission Study of the Morphology and Barrier Heights at the Interface between Benz[a]anthracene and Noble Metal (111) Surfaces

K. Manandhar† and B. A. Parkinson*

Department of Chemistry, School of Energy Resources, University of Wyoming, Laramie, Wyoming 82071, United States

ABSTRACT: Various coverages of benz[a]anthracene (BA) thin films prepared by depositing the molecules in several steps on Au(111) and Ag(111) were investigated using ultraviolet and X-ray photoelectron spectroscopy (UPS and XPS). XPS and UPS were taken after each deposition. A Schottky junction formed between BA/Au(111) and BA/Ag(111). A hole barrier height of 1.89 eV in BA/Ag(111) was determined directly from the observed highly occupied molecular orbital (HOMO) peak cutoff however a HOMO peak cutoff in BA/Au(111) 1.63 eV was indirectly determined. When combined with previous measurements of the BA/Cu(111) interface, the slope S of the plot of hole barrier height as a function of metal workfunction (WF) was calculated to be 0.39, which is close to the S value of pentacene. Discussion on film growth mode, band bending, band diagram, and comparisons of interface parameter S of BA with S of other molecules condensed on metal surfaces are presented.

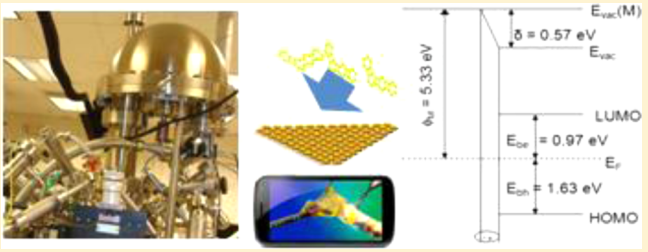

1. INTRODUCTION

Organic molecules are prospective future semiconductor materials for cost-effective electronic and opto-electronic devices. Recently, applications of organic thin film electronic and opto-electronic devices, such as organic thin film transistors (OTFTs), organic light emitting diodes (OLEDs), and organic photovoltaics (OPVs) in commercial products have been very rapidly increasing. These devices all employ multiple layers of organic materials and usually metal contacts for electron or hole injection. Electrical characteristics of the organic/metal contacts depends on electron and the hole barriers, the energy differences of the highest occupied molecular orbitals (HOMO) and the lowest unoccupied molecular orbital (LUMO) of the organic film with respect to the metal Fermi level (FL). These barriers are of prime importance as they determine the key parameters of device operation such as driving voltages for OLEDs and photovoltages of OPV devices. Despite their obvious importance and decades of research focusing on organic semiconductor/metal junctions,[1−9] the electrical characteristics of organic/metal interfaces is still unpredictable.

Polyaromatic hydrocarbons (PAHs) are the front runner in choice as a versatile semiconductor material for application in many lower performance and cost-effective devices where amorphous silicon is currently employed.[10] Benz[a]anthracene (BA) (Figure 1 inset) is a planar PAH molecule consisting of four fused benzene rings that is chiral when confined to a planar surface. Recently, our group has investigated the interface electronic properties and thin film structure of BA molecule on Cu(111) surfaces employing photoelectron spectroscopies (UPS and XPS) and scanning tunneling microscopy (STM).[11] The UPS and XPS results showed that the growth mode of BA molecular film is classical Stranski−Krastnov (SK) type similar to the growth mode of the majority of PAHs on the weakly interacting substrates.[11−15] The UPS study further showed the hole barrier height (E_{bh}) of 1.78 eV,[11] which is similar to the E_{bh} of its isomer chrysene.[14] The energetics of BA/Au(111) and BA/Ag(111) interfaces, to our knowledge, have yet not been studied. In this contribution, we measure the energy level alignment for BA on Au(111) and Ag(111) using XPS, UPS and ultraviolet and visible (UV−vis) spectroscopy and, combined with our previous measurements of the BA on Cu(111) interface,[11] we estimate the interface parameter S from the plot of barrier height as a function of metal workfunction (WF).

2. EXPERIMENTAL SECTION

Experiments were performed in a commercial Omicron Multiprobe ultrahigh vacuum (UHV) system (base pressure 8 × 10^{-10} Torr). This system is equipped with a variable temperature STM (VT-STM) for surface structural characterization. XPS and UPS, using a VSW EA125 single channel hemispherical analyzer, were used to study the electronic structure of the interface. A physical vapor deposition chamber (base pressure 1 × 10^{-8} Torr) is attached to the UHV system allowing samples and films to be prepared in situ.

The silver and gold films were prepared in the load lock of the vacuum chamber by evaporating silver or gold onto freshly cleaved mica. The micas were outgassed overnight at around

Received: June 18, 2012
Published: August 7, 2012

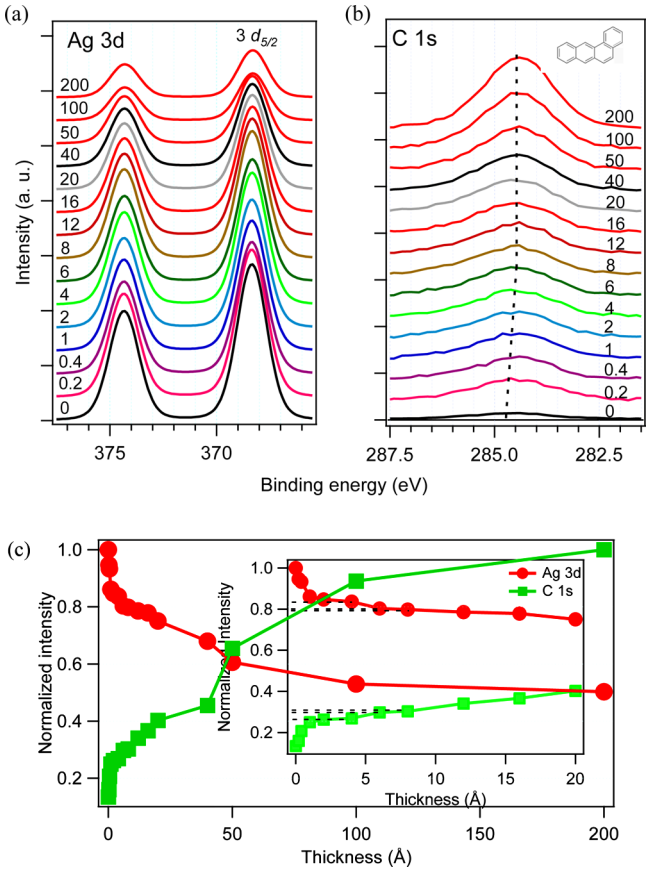

Figure 1. (a, b) Ag 3*d* and C 1*s* XPS spectra for indicated thicknesses of BA films. (c) Graph of the normalized integrated area intensities for the Ag 3*d* and the C 1*s* emissions as a function of BA thickness.

410 °C and held at temperature between 300 and 250 °C during silver and gold evaporation, respectively. The deposition rates, as monitored by quartz crystal growth monitor, were about 120 and 37 Å/min for silver and gold, respectively. The silver and gold films were approximately 500 Å and 700 Å thick, respectively. Cycles of sputtering at 1 keV energy with Ar-partial pressure of 7×10^{-7} Torr and annealing at 400 °C were used to clean and flatten the Au(111) and Ag(111) surfaces. The chemical purity of the surface was determined with XPS (Mg kα, 50 eV pass energy) and the presence of flat surfaces was confirmed with STM.[16] The surfaces revealed terraces as large as 600 × 500 nm and 550 × 400 nm with monatomic step heights of 2.27 and 2.30 Å in silver and gold surfaces, respectively, which are within 4% error from the accepted values of 2.36 Å for both Au(111) and Ag(111).

BA (Aldrich Chemical Co.) films were prepared in deposition chamber using a silicone rubber flexible heater to resistively heat a quartz ampule prepared from a UHV series quartz-metal adapter (source temperature, ~110 °C). The source was extensively degassed at about 100 °C prior to deposition. The quartz ampule containing BA was heated to obtain a desired deposition rate that was monitored by a Leybold quartz crystal microbalance (QCM). The deposition rate was on average 1.5 monolayer(ML)/min with 1 ML is defined as a thickness of 6 Å as measured by the QCM. The Ag(111) and Au(111) substrate were maintained at room temperature (RT) during the deposition.

Sequential depositions were performed on silver and gold substrates up to a final film thickness of 200 Å and 450 Å, respectively. After each growth step, XPS and UPS (HeI, 21.21 eV; with 10 eV pass energy) were utilized to measure the electronic structure of the surface. XPS spectra were taken with a takeoff angle of ~20° from the normal emission, while UPS spectra were collected under normal emission. A −10.00 V bias was applied to the sample for the UPS measurements to separate the sample and spectrometer high binding energy cutoffs (HBECs). The spectrometer was calibrated as previously described.[17] WF and HOMO-cutoff positions were determined from the HBECs and HOMO onsets, respectively, of UP spectra. XPS core level peak positions were determined by a fitting routine using IGOR Pro (Wavemetrics) data evaluation software. A vacuum deposited BA film on quartz was used to obtain the thin film solid-state absorption spectrum that was measured using a Varian Cary−500 UV−Vis−NIR spectrophotometer.

3. RESULTS AND DISCUSSION

3.1. XPS of BA on Silver and Gold. The XPS experimental results from deposition of BA onto Au(111) is very similar to those obtained for the Ag(111) system. Therefore, we will only present the detailed experimental data for the BA/Ag(111) system. Ag 3*d* and C 1*s* XPS spectra for various thicknesses of BA films are shown in Figure 1(a,b), respectively. The BEs of the Ag $3d_{5/2}$ emission, obtained after a careful fitting procedure, is constant at 368.34 eV for all deposition steps (Figure 1a). Initially, the C 1*s* BE associated with small amount of contamination on Ag(111) surface is 284.74 eV[13−15] (Figure 1b). For the initial BA deposition, the BE gradually reduces and remains unchanged within 0.05 eV at 284.47 eV starting from a thickness of 6 Å up to a thickness of 200 Å (Figure 1b).

Figure 1c is a graph of the normalized integrated area intensities for the Ag 3*d* and the C 1*s* emissions as a function of BA thickness. The intensities were normalized to the peak area of the most intense peaks of Ag 3*d* and C 1*s* emissions. Initially, the Ag 3*d* emission is strongly suppressed, while a large increase in C 1*s* intensity is measured. After depositing approximately 6 Å, the C 1*s* intensity was ~27% of its eventual maximum whereas the Ag 3*d* was 78% of its initial value (Figure 1c, inset). It is noticeable that at very long deposition times, only a small further decrease in substrate intensity occurs.

3.2. UPS of BA on Silver and Gold and HOMO and LUMO Cutoff Determination. Figures 2 and 3 show the UP-spectra data of BA deposition onto silver and gold surfaces, respectively. Figure 2a−c shows the HBC, BA spectral, and HOMO spectral regions of BA on silver surface, respectively, and Figure 3a−c shows the full spectra, HBC region, and BA spectral region of BA on gold surface, resepctively. The clean Ag(111) and Au(111) surfaces show the expected Ag 4*d* (full spectra showing Ag 4*d* valence band is not presented) and Au 5*d* (Figure 3a) valence bands, respectively. Subsequent deposition of the aromatic molecules gradually suppresses the valence states. The emission signal just below the FL forms almost a flat continuum band as the photoionization cross section of outmost *s*-subshell of silver and gold is much smaller than those of the *d*-subshells[18,19] (see Figures 2c and 3a). For the clean Ag(111) and Au(111) surfaces, the WFs were measured to be 4.73 and 5.33 eV, respectively (Figures 2a and 3b) which agree within experimental error with the literature values 4.74 and 5.31 eV, respectively.[20−22] The shift in WF as a function of BA film thickness is plotted in Figures 2d and 3d. Upon deposition of about 6 Å of BA, the WF of the silver and

dx.doi.org/10.1021/jp305998b | J. Phys. Chem. C 2012, 116, 19379−19384

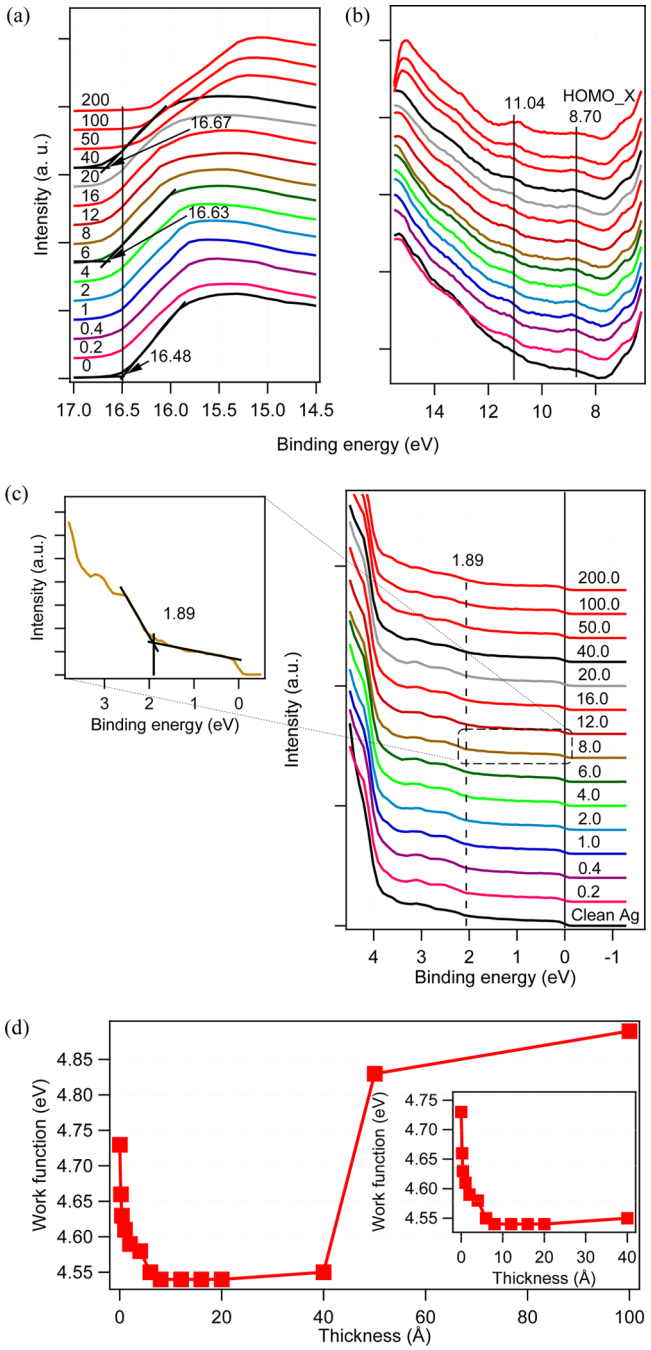

Figure 2. (a, b and c) High binding energy cutoff (HBEC), BA spectral and HOMO cutoff region UPS spectra for indicated thickness of BA on the Ag(111) surface, (d) Plot of work function of Ag(111) versus BA thickness and the insert is the plot for BA thickness up to 40 Å.

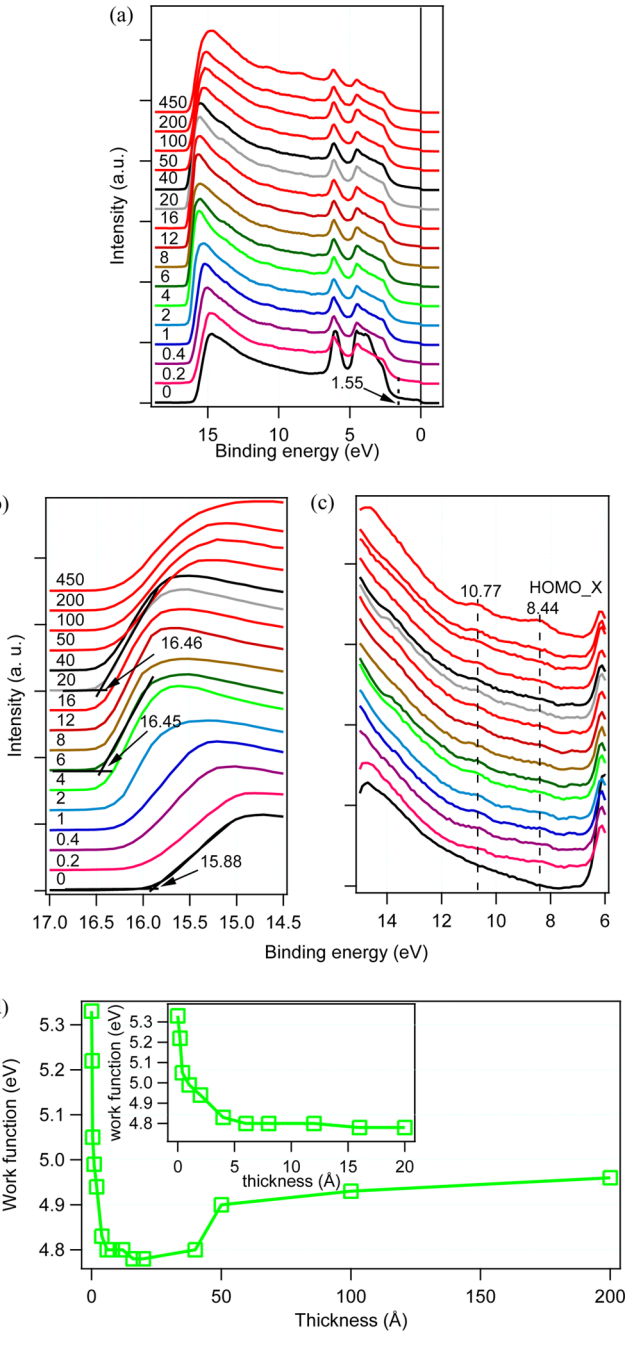

Figure 3. (a, b and c) Full, BA spectral region and HOMO cutoff region UPS spectra for indicated thickness of BA on the Au(111) surface, (d) Plot of work function of Au(111) versus BA thickness and the insert is the plot for BA thickness up to 20 Å.

gold were measured 4.58 eV (Figure 2a,d) and 4.76 eV (Figure 3b,d), respectively. The silver and gold WFs are unchanged within ±0.04 eV for BA thickness up to 40 Å and within ±0.02 eV for BA the thickness up to 20 Å, respectively (Figures 2a,d and 3b,d). The silver and the gold WFs gradually increase when BA thicknesses are thicker than 40 Å and 20 Å, respectively (Figures 2a,d) and 3b,d). This change in WF, with no change in HOMO_X position (discussed below), implies a change in the ionization potential of molecular film. This change in WF may originate from a change in BA orientation.[15,23,24]

The offset between the HOMO cutoffs of the BA and the metal FL is of interest because it represents the height of the hole injection barrier (E_{bh}) at the interfaces. Figure 2c is the HOMO spectral region of BA deposition on silver surface. In the spectra stacked graph, HOMO peaks being weak are not observed. A close examination of the photoemission onset region of a spectrum reveals the HOMO and the HOMO cutoff is measured at BE 1.89 eV (Figure 2c). However, in BA/Au(111) spectra, HOMO peaks are not revealed even in close examination. We assume BA HOMO peaks in BA/Au(111) are not revealed due to overlap of the growing weak HOMO levels of BA with intense gold 5*d* states. This fact is clearly observed

dx.doi.org/10.1021/jp305998b | J. Phys. Chem. C 2012, 116, 19379−19384

when we carefully examine the flat continuum bands of outmost *s*-subshell of silver and gold (Figures 2c and 3a). This band extends up to ∼3.20 eV in silver while it extends to ∼1.55 eV in gold (Figure 3a). Therefore, intense low BE Au *d*-band which begins at ∼1.55 eV overlaps the weak BA HOMO at ∼1.63 eV (calculation presented below). To further verify that a weak BA HOMO is revealed if a strong emission of substrate is absent at around HOMO region, UPS investigations of BA films on highly oriented pyrolytic graphite (HOPG) substrate were performed, as HOPG does not have strong emissions in the BE range below 11 eV (Figure 4). The characteristic

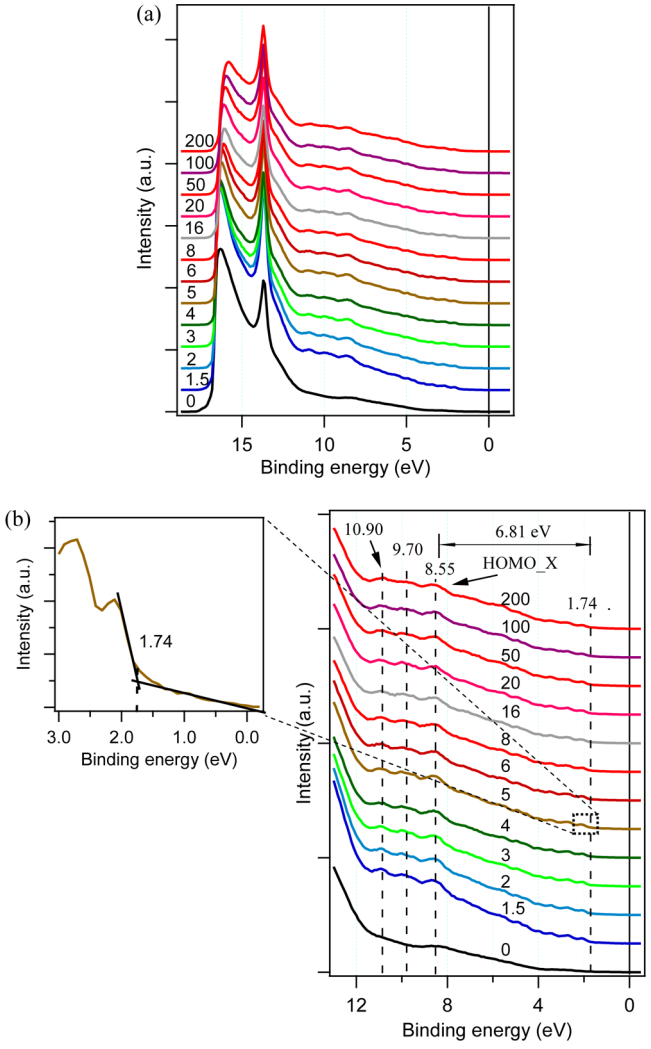

Figure 4. (a and b) Full and HOMO_X consisting BA spectral region UPS spectra for indicated thickness of BA on HOPG.

featureless UPS spectrum of bare HOPG below 11 eV is given in Figure 4a.[11,14] As expected immediately after the first deposition step (see Figure 4a,b), a HOMO and a number of new emissions appear that grow only slightly after the initial deposition step and exhibit no shape change for films up to 200 Å thick. A close examination of the photoemission onset allows for the determination of the HOMO cutoff position at a BE of 1.74 eV (Figure 4b). This proves that the invisibility of the weak HOMO in the BA/Au(111) system is in fact due to overlap of it with the intense Au 5*d* valence band. Therefore, the HOMO cutoff for BA/Au(111) system was indirectly estimated. It is noteworthy that the other HOMOs labeled HOMO_Xs of BA/Ag(111) and BA/HOPG (Figures 2b and 4b) are at 8.70 and 8.55 eV, respectively. Molecule's HOMO and HOMO_X emission BEs do not change in the spectra of subsequently deposited BA film onto both HOPG and Ag(111). Further, the difference between the first HOMO_X emission and the HOMO cutoff in BA/Ag(111) and BA/HOPG is 6.81 eV (Figures 2b,c and 4b). This is consistent with the observed constant energy difference of HOMO_X and the HOMO cutoff, 7.3 ± 0.1 and 7.5 ± 0.1 eV for perylene[12,13] and pentacene,[15,17] respectively, after deposition onto Ag(111), Cu(111), and Au(111) surfaces. The constant energy difference between HOMO_X and the HOMO cutoff for a molecular film deposited onto different substrate is regarded as a property of the molecule.[14,25] Assuming the energy difference between HOMO_X and HOMO cutoff of BA is same irrespective of onto which surface it is deposited, a BE of HOMO cutoff for the BA films onto Au(111) is calculated. The HOMO cutoffs were calculated to be 1.63 eV (8.44−6.81 eV = 1.63 eV) for the BA films onto Au(111).

LUMO cutoff of BA film can be estimated by measuring BA bandgap (HOMO−LUMO gap). The BA bandgap of 2.6 eV is obtained from UV−vis (Figure 5a). (It is important to note that the first excitonic transition is only used as an estimate for the HOMO−LUMO gap because the large excitonic BE of the molecule and the polarization effects[25] are not accounted for.)

3.3. Film Growth Mode and Band Bending. The decrease in the rate of change of Ag 3*d* intensities in the intermediate coverages of silver, and the still discernible substrate signals after deposition of 200 Å of BA (Figure 1c), is consistent with a growth mode where a formation of wetting layer of BA is initially formed, followed by island growth (classic SK growth mode).[14] Therefore, regions with less than 2 ML, the approximate escape depth for photoemitted electrons,[25] must exist even for the thick BA films and the wetting layer most likely contains only a single ML of BA. The fact wetting of the surface likely with single ML of BA is further supported by observations of the constant BE of BA C 1*s* emission starting from thickness of ∼6 Å (Figure 1b), a noticeable change in Ag 3*d* intensity starting from thickness of ∼6 Å of BA (Figure 1c), the significant change of the Ag(111) and Au(111) WFs when BA film thickness increases from sub-ML to ∼6 Å thick (Figures 2a,d and 3b,d) and unchanged WFs with further addition of BA to thicknesses up to ∼40 and ∼20 Å on silver and gold substrates, respectively.

Band bending occurring in the organic material, or polarization energy-related shifts at the interface were determined by measuring the shift of the core level photoemission peaks. The Ag 3*d* is not subject to any band bending-related shifts, so as expected Ag $3d_{5/2}$ BE was measured constant at 368.34 eV (Figure 1a).[26] As discussed above, there were no shifts in the BA C 1*s* binding energy. Also the HOMO cutoff in BA/Ag(111) observed at 1.89 eV and the distinct BA emission features observed at 8.44 and 10.77 eV and 8.70 and 11.04 eV in BA/Au(111) and BA/Ag(111), respectively, after the first deposition step in the UP-spectra maintained a consistent value (Figures 2b and 3c). This observation corroborates the BA C 1*s* core level XPS results. Since there are no detectable BE shifts in the BA features in the UP-spectra and no BE shifts in BA C 1*s* in XPS, band bending can be excluded.

3.4. Band Diagram and Interface Properties. With the information of HOMO cutoff positions, bandgap, and the WFs of the clean Ag(111) and Au(111) surfaces (4.73 and 5.33 eV,

dx.doi.org/10.1021/jp305998b | J. Phys. Chem. C 2012, 116, 19379−19384

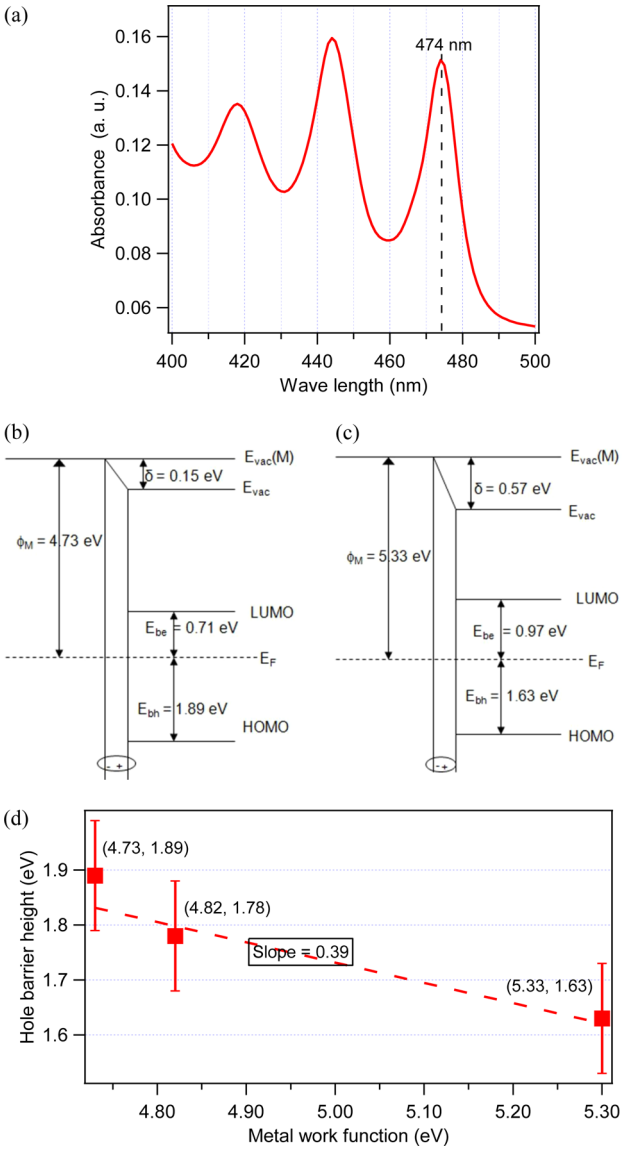

Figure 5. (a) Visible absorption spectrum of BA, (b and c) band diagram of BA/Ag(111) and BA/Au(111), (d) plot of interface parameter *S*, hole barrier height (E_{bh}) versus metal work function (φ_M).

respectively) and of the surfaces with 6 Å thick BA films (4.58 and 4.76 eV, respectively), which just entirely covers the substrates, on them, band diagrams for BA/Ag(111) and BA(Au(111), respectively, can be drawn as shown in Figure 5b,c. Due to the absence of band bending, the difference of WFs directly translate into an interface dipole potentials of δ = 0.15 (4.73−4.58) and 0.57 eV (5.33−4.76) for BA and Ag(111) and Au(111) interfaces, respectively (Figure 5b,c). From the energy level diagram, it is evident that the interface dipoles are pointing from molecules into the substrate. Similarly, interface dipole for BA and HOPG interface was calculated to be −0.26 eV and it is pointing from the substrate into the molecule.[11]

The interface parameter *S* gives the magnitude of the change of barrier height as a function of the WF of the contacting metal. Combined with previous measurements of the BA/Cu(111) interface,[11] the slope *S* of the plot of hole barrier height as a function of metal workfunction (WF) was calculated to be 0.39 (Figure 5d). An *S* = 1, the Schottky-limit for inorganic semiconductor interfaces, would be expected for the weakly interacting interfaces formed by organic solids. The *S* values of different PAHs when deposited on metal surfaces ranges from Bardeen (*S* = 0) to nearly Schottky (*S* ≈ 1) limit (Table 1). The planar PAHs without heteroatoms demonstrated *S* values ranging from 0 to 0.56. (e.g., Chrysene[14] *S* = 0, pentacene[15,27] *S* = 0.37, and perylene[12,13] *S* = 0.56. The planar heteroatomic PAHs, the *S* values ranges from 0 to 0.6, e.g., 3,4,9,10-perylene-tetracarboxylicacid-dianhydride (PTCDA)[27] *S* = 0, *N*,*N*′-diphenyl-*N*,*N*′-bis(1-naphthyl)-1,1′biphenyl-4,4′′diamine (α-NPD)[28] *S* = 0.49 4,4′-*N*,*N*′-dicarbazolyl-biphenyl (CBP)[28] *S* = 0.6. The *S* values of bulky three-dimensional molecules tris(8-hydroxyquinolino)aluminum (Alq_3)[28] (*S* ≈ 0.9) and *N*,*N*′-bis(1-naphyl)-*N*,*N*′diphenyl-1,1′-biphennyl-4,4′-diamine (NPB)[29] (*S* ≈ 0.6) are well above zero. The *S* value 0.39 of BA is close to the *S* value of pentacene but smaller than the *S* values for similar PAHs without heteroatom such as perylene. Also, this *S* value is larger than the *S* value of planar heteroatomic PAHs PTCDA but smaller than the *S* value of other planar heteroatomic PAHs and smaller than the *S* value of all of the bulky three-dimensional molecules. Overall, the ranges of the *S* values for planar PAHs with and without heteroatoms are different from the three-dimensional heteroatomic PAHs. This might be due to difference of morphology of the films formed and to the difference in an intimate contact these spatially different structure molecules form with the substrate surface. As yet, there is not any basis to reliably predict the *S* value for metal-PAH systems. This obviously deserves more systematic photoelectron spectroscopy, X-ray standing wave measurement (XSW) along with STM studies (first, molecules only containing carbon and second, molecules with other elements such as, e.g., O and N and third various three-dimensional PAHs). It is noteworthy, however, for in situ prepared transition-metaloxides-PAHs systems, Greiner et al. recently reported consistent energy alignment trend.[30] The metaloxide-PAHs contact approaches the Schottky limit when metaloxide WF is smaller than adsorbed PAH ionization energy and it starts approaching Bardeen limit when metaloxide WF is equal to PAH ionization energy. Therefore, the authors further claim that the substrate band structure (position of valence and conduction band of metaloxide with respect to HOMO of the PAHs) does not affect the equilibrium energy alignment position of adsorbed molecules. Rather, energy alignment is governed by the equilibration of substrate's

Table 1. Interface Parameter *S* of Different Geometric Structure PAHs

PAH types	without-heteroatom-planner	planar-heteroatom	3-D
molecules = *S* value	chrysene = 0[14]	3,4,9,10-perylene-tetracarboxylicacid-dianhydride (PTCDA) = 0[27]	tris(8-hydroxy-quinoline)aluminum (Alq_3) = 0.90[28]
	pentacene = 0.37[15,27]	*N*,*N*′-diphenyl-*N*,*N*′-bis(1-naphthyl)-1,1′-biphenyl-4−4′-diamine (α-NPD) = 0.49[28]	*N*,*N*′-bis(1-naphyl)- *N*,*N*′diphenyl-1, 1′-biphennyl-4,4′-diamine (NPB) = 0.60[29]
	perylene =0.56[12,13]	4,4′-*N*,*N*′-dicarbazolyl-biphenyl (CPB) = 0.60[28]	

dx.doi.org/10.1021/jp305998b | J. Phys. Chem. C 2012, 116, 19379−19384

electron potential with an adsorbed molecule's oxidation/reduction potentials.

For understanding the Schottky barrier formation and FL pinning at nonreacting organic semiconductor/metal interfaces, Vazquez et al. have extended the concepts of an induced density of interface states (IDIS) and the theory describing the charge neutrality level (CNL) initially developed for inorganic semiconductor interfaces.[31,32] The authors demonstrated that even for weakly interacting systems there are IDIS in the gap of the organic material, which can explain the observed dipoles, FL pinning and energy level alignment.[31,32] They attributed the small value of S to a larger density of states induced in the organic band gap limiting tendency of the interface FL to move within the organic energy gap. The smaller value $S = 0.39$ for BA film on noble metal (111) surface implies the IDIS in these systems is not yet large enough to pin the FL at the organic CNL.

4. CONCLUSIONS

We investigated thin films of BA on Au(111) and Ag(111) using UPS and XPS. The UPS and XPS spectra indicated that at approximately 6 Å thickness a wetting layer of BA was formed followed by island growth. The constant BE of C 1*s* core level emissions in XPS and BA emissions in UPS provided no evidence of band bending in BA-Au(111) and and BA-Ag(111). The band line up of BA on Au(111) and Ag(111) illustrated that a Schottky barrier is formed between these materials with hole injection barriers of 1.63 and 1.89 eV, respectively. In BA/Au(111) and BA/Ag(111), interface dipoles of 0.57 and 0.15 eV, respectively, were measured at the 6 Å BA covered interface. The calculated S value of 0.39 is close to the S value of pentacene but smaller than the S values for similar PAHs without heteroatom such as perylene. This S value is larger than the S value of planar heteroatomic PAHs PTCDA but smaller than the S value of other planar heteroatomic PAHs and smaller than the S value of all the bulky three-dimensional molecules. As yet, there is not any basis to reliably predict the S value.

AUTHOR INFORMATION

Corresponding Author

*Tel: +1 307 766 4363; fax: +1 307 766 2807; e-mail : bparkin1@uwyo.edu.

Present Address

†Department of Chemistry, University of Illinois at Chicago. E-mail: dhamma11@uic.edu.

Notes

The authors declare no competing financial interest.

ACKNOWLEDGMENTS

This work was supported by University of Wyoming startup funds.

REFERENCES

(1) Schottky, W. *Z. Phys. Chem.* **1939**, *45*, 33.
(2) Bardeen, J. *Phys. Rev.* **1947**, *71*, 717.
(3) Louie, S. G.; Chelikowsky, J. R.; Cohen, M. L. *Phys. Rev. B* **1977**, *15*, 2154.
(4) Brillson, L. J. *Phys. Rev. Lett.* **1978**, *40*, 260.
(5) Tersoff, J. *Phy. Rev. B* **1984**, *30*, 4874.
(6) Jaegermann, W.; Pettenkofer, C.; Parkinson, B. A. *Phys. Rev. B* **1990**, *42*, 7487.
(7) Tung, R. T. *J. Vac. Sci. Technol. B* **1993**, *11*, 1546.
(8) Monch, W. *Appl. Phys. Lett.* **1998**, *72*, 1899.
(9) Tung, R. T. *Phys. Rev. Lett.* **2000**, *84*, 6078.
(10) Anthony, J. E. *Angew. Chem. Int. Ed.* **2008**, *47*, 452.
(11) Manandhar, K.; Parkinson, B. A. *J. Phys. Chem. C* **2011**, *115*, 5910.
(12) Manandhar, K.; Parkinson, B. A. *J.Phys. Chem. C* **2010**, *114*, 15394.
(13) Manandhar, K.; Sambur, J. B.; Parkinson, B. A. *J. Appl. Phys.* **2010**, *107*, 063716.
(14) Jaeckel, B.; Sambur, J.; Parkinson, B. A. *J. Phys. Chem. C* **2009**, *113*, 1837.
(15) Jaeckel, B.; Sambur, J. B.; Parkinson, B. A. *J. Appl. Phys.* **2008**, *103*, 063719.
(16) Barth, J. V.; Brune, H.; Ertl, G.; Behm, R. J. *Phys. Rev. B* **1990**, *42*, 9307.
(17) Schroeder, P. G.; France, C. B.; Park, J. B.; Parkinson, B. A. *J. Phys. Chem. B* **2003**, *107*, 2253.
(18) Becke, A. D. *J. Chem. Phys.* **1993**, *98*, 5648.
(19) Ertl, G.; Küppers, J. *Low Energy Electrons and Surface Chemistry*; VCH Verlagsgesellschaft: Weinheim, 1985.
(20) Salaneck, W. R.; Seki, K.; Kahn, A.; Pireaux, J.-J. *Conjugated Polymer and Molecular Interfaces*; Marcel Dekker, Inc.: NY, 2002.
(21) Cardona, M., Ley, L. *Photoemission in Solids*; Springer-Verlag: Berlin, 1978; Vols. *1* & *2*, p 1979.
(22) Holzl, J. and . Shulte, F. K. *Work Function of Metals in Solid Surface Physics*; Springer-Verlag: Berlin, 1979.
(23) Koch, N.; Vollmer, A.; Duhm, S.; Sakamoto, Y.; Suzuki, T. *Adv. Mater.* **2007**, *19*, 112.
(24) Duhm, S.; Heimel, G.; Salzmann, I.; Glowatzki, H.; Johnson, R. L.; Vollmer, A.; Rabe, J. P.; Koch, N. *Nat. Mater.* **2008**, *7*, 326.
(25) Amy, F.; Chan, C.; Kahn, A. *Org. Electron.* **2005**, *6*, 85.
(26) France, C. B.; Schroeder, P. G.; Forsythe, J. C.; Parkinson, B. A. *Langmuir* **2003**, *19*, 1274.
(27) Kahn, A.; Koch, N.; Gao, W. Y. *J. Polym. Sci., Part B: Polym. Phys.* **2003**, *41*, 2529.
(28) Hill, I. G.; Rajagopal, A.; Kahn, A.; Hu, Y. *Appl. Phys. Lett.* **1998**, *73*, 662.
(29) Lee, C. S.; Tang, J. X.; Zhou, Y. C.; Lee, S. T. *Appl. Phys. Lett.* **2009**, *94*, 3.
(30) Greiner, M. T.; Helander, M. G.; Tang, W.-M.; Wang, Z.-B.; Qiu, J.; Lu, Z.-H. *Nat. Mater.* **2012**, *11*, 76.
(31) Vazquez, H.; Flores, F.; Oszwaldowski, R.; Ortega, J.; Perez, R.; Kahn, A. *Appl. Surf. Sci.* **2004**, *234*, 107.
(32) Vazquez, H.; Flores, F.; Kahn, A. *Org. Electron.* **2007**, *8*, 241.